Pharm Res (2011) 28:2530–2542
DOI 10.1007/s11095-011-0481-y

RESEARCH PAPER

Population PK and IgE Pharmacodynamic Analysis of a Fully Human Monoclonal Antibody Against IL4 Receptor

Tarundeep Kakkar • Cynthia Sung • Leonid Gibiansky • Thuy Vu • Adimoolam Narayanan • Shao-Lee Lin • Michael Vincent • Christopher Banfield • Alex Colbert • Sarah Hoofring • Marta Starcevic • Peiming Ma

Received: 18 January 2011 / Accepted: 13 May 2011 / Published online: 21 May 2011

ABSTRACT

Purpose For AMG 317, a fully human monoclonal antibody to interleukin receptor IL-4Rα, we developed a population pharmacokinetic (PK) model by fitting data from four early phase clinical trials of intravenous and subcutaneous (SC) routes simultaneously, investigated important PK covariates, and explored the relationship between exposure and IgE response.

Methods Data for 294 subjects and 2183 AMG 317 plasma concentrations from three Phase 1 and 1 Phase 2 studies were analyzed by nonlinear mixed effects modeling using first-order conditional estimation with interaction. The relationship of IgE response with *post hoc* estimates of exposure generated from the final PK model was explored based on data from asthmatic patients.

Results The best structural model was a two-compartment quasi-steady-state target-mediated drug disposition model with linear and non-linear clearances. For a typical 80-kg, 40-year subject, linear clearance was 35.0 mL/hr, central and peripheral volumes of distribution were 1.78 and 5.03 L, respectively, and SC bioavailability was 24.3%. Body weight was an important covariate on linear clearance and central volume; age influenced absorption rate. A significant treatment effect was observable between the cumulative AUC and IgE response measured.

Conclusion The population PK model adequately described AMG 317 PK from IV and SC routes over a 60-fold range of doses with two dosing strengths across multiple studies covering healthy volunteers and patients with mild to severe asthma. IgE response across a range of doses and over the sampling time points was found to be related to cumulative AMG 317 exposure.

KEY WORDS asthma · IL-4Rα · monoclonal antibody · pharmacodynamics · pharmacokinetics

Electronic Supplementary Material The online version of this article (doi:10.1007/s11095-011-0481-y) contains supplementary material, which is available to authorized users.

T. Kakkar (✉) • T. Vu • A. Narayanan • A. Colbert • P. Ma
Department of Pharmacokinetics and Metabolism, Amgen Inc.
Thousand Oaks, California 91320, USA
e-mail: tkakkar@amgen.com

C. Sung
Rainbow Pharma Consulting, Pte. Ltd.
Singapore, Singapore

L. Gibiansky
QuantPharm LLC
North Potomac, Maryland, USA

S.-L. Lin
Department of General Medicine & Inflammation, Amgen Inc.
Thousand Oaks, California 91320, USA

M. Vincent • C. Banfield
Department of Early Development, Amgen Inc.
Thousand Oaks, California 91320, USA

S. Hoofring • M. Starcevic
Department of Clinical Immunology & BSM, Amgen Inc.
Thousand Oaks, California 91320, USA

INTRODUCTION

The cytokines IL-4 and IL-13 play a central role in the initiation and maintenance of inflammatory lung disease. The effects of IL-4 and IL-13 include immunoglobulin class switching in B-cells and stimulation of IgE production, goblet cell hyperplasia and mucus hypersecretion, induction

of chemokine production from fibroblast and epithelial cells, promotion of eosinophilic infiltration and airway hyper-responsiveness (1). On many cell types, biological responses to IL-4 and IL-13 are mediated through the same heterodimeric receptor IL-4Rα. Supportive evidence has been established through experiments in mice deficient in one or both of these cytokines (2–4). Mice deficient in IL-4Rα (knockout mice) fail to develop an asthma-like phenotype when antigen challenged. In addition, these knockout mice fail to elicit a response even after the administration of IL-4, IL-13, and Th2 cells in the presence of antigen (2,5). Studies of human genetic polymorphisms of IL-4R suggest that variants with increased function result in an elevated risk of asthma or increased IgE serum titers (6–9). Taken together, these studies suggest that IL-4Rα is a suitable target for pharmacological blockade in search for new treatments of asthma and that IgE levels are a mechanistically relevant biomarker for effect.

AMG 317 is a fully human IgG_2 monoclonal antibody that binds with high affinity to human IL-4Rα (K_d= 0.18 nM). In an *in vitro* functional assay, AMG 317 inhibited IL-4- and IL-13-induced expression of the low affinity IgE receptor CD23 on human B-cells with IC_{50} values of 0.16 and 0.25 nM, respectively. It also blocks IL-4 and IL-13 induction of the cytokines TARC, MCP-4 and eotaxin-3 in a concentration-dependent manner. As its activity on IL-4Rα is limited to humans and chimpanzees, surrogate molecules were developed to evaluate the biologic activity and safety of IL-4Rα antibodies in mouse models of asthma. An anti-murine IL-4R chimeric antibody, murine AMG 317, inhibits muIL-4 and muIL-13 in a murine B9 cell proliferation assay with IC_{50} values of 0.075 and 0.13 nM, respectively. In ovalbumin (OVA)-sensitized BALB/c and C57BL/6 mice, pretreatment with murine AMG 317 at the time of OVA challenge resulted in reduced accumulation of eosinophils in the lung, decreased mucus production, reduced Th2 cytokine levels from draining lung lymph nodes and lowered total serum IgE relative to a control immunoglobulin. In a mouse model of chronic asthma (cockroach allergen rechallenge model), treatment with murine AMG 317 by IV administration reduced lung inflammation, airway hyper-responsiveness to inhaled methacholine, total serum IgE, and accumulation of lung hydroxyproline, an amino acid unique to collagen that is indicative of lung remodeling. Based on these and other preclinical findings and supportive toxicological assessments, a clinical program of the human antibody AMG 317 was undertaken.

AMG 317 has now been studied in three phase 1 trials and one phase 2 trial (10) to evaluate the safety, tolerability, pharmacokinetics (PK), and pharmacodynamics (PD) of single or multiple weekly doses given by intravenous (IV) or subcutaneous (SC) injection. The phase 1 trials were conducted in healthy volunteers and patients with mild to moderate asthma; the phase 2 trial was conducted in patients with moderate to severe asthma. Here we present a population PK model of AMG 317 that was developed by simultaneously modeling of both IV and SC data. The dataset included 2183 concentrations from 294 subjects. A two-compartment quasi-steady-state (QSS) pharmacokinetic model, as an approximation to the general target-mediated drug disposition (TMDD) model, with linear and nonlinear clearances described the entire range of observed data. The PK model was used to determine bioavailability, identify important PK covariates, and establish an exposure-response relationship with IgE levels, which are indicative of Th2 pathway activity and related to disease activity in asthma.

MATERIALS AND METHODS

Patient Population and Study Design

Four studies contributed data for the population analysis. Study A was a single dose, dose-escalation study (IV 10–1000 mg, SC 100–300 mg) in healthy volunteers or adults with mild to moderate persistent asthma. Study B was a multiple-dose, dose-escalation study (SC 75, 150, 300 or 600 mg) administered once weekly for four consecutive weeks to adults with mild to moderate asthma. Study C was a single 150 mg SC dose study administered to adolescents (12 to 18 years) and adults with mild to moderate persistent asthma. Subjects in the above three Phase 1 studies, which were conducted at one or two centers, had intensive PK sampling at 0 (predose), and approximately at 0.5, 1, 2, 4, 8, 12, 24 h, daily for subsequent 7 days and on days 10, 14, 21 (additional 0.5, 1, 2, 4, 8, 12 and 24 h for Study B), 28, 35, 42, and 56 after the first dose. In the Phase 2 study conducted in 52 centers (Study D), SC doses (75, 150 or 300 mg) were administered once weekly by subcutaneous injection for 12 consecutive weeks to adults with moderate to severe asthma. Most subjects in this study had sparse sampling, predose at 0 and at weeks 4, 8, 12 and 16; a subset of 32 subjects had up to 6 additional blood samples drawn. Patient demographics and characteristics of the treatments are shown in Table I. The final population PK dataset contained data from 294 patients and 2183 concentrations. The final population PD dataset contained data from 281 patients and 1069 IgE concentration levels. The IgE samples in intensively sampled studies were collected in weeks 0 (baseline and day 1), 1, 3, 4, 5, 6 and 8. In the Phase 2 study, most of the sparse IgE samples were collected in weeks 0, 4, 8, 12, and 16.

Table 1 Characteristics of Patients and Treatments Included in Population PK Analysis ($N = 294$)

	Category	N	%
Study No.	A	60	20.4%
	B	24	8.2%
	C	18	6.1%
	D	192	65.3%
Sex	Male	168	57.1%
	Female	122	41.5%
	Missing	4	1.4%
Race	White	218	74.1%
	Black	35	11.9%
	Hispanic	14	4.8%
	Japanese	12	4.1%
	Asian	7	2.4%
	Other[a]	8	2.7%
Health Status	Healthy	47	16.0%
	Mild or Moderate Asthmatic	247	84.0%
Route of Administration	IV	29	9.9%
	SC	265	90.1%
Formulation	F0: 30 mg/mL	54	18.4%
	F1: 100 mg/mL	234	79.6%
	F2: 100 mg/mL diluted to 30 mg/mL	6	2.0%
Dose Regimen (Dose/Route/ Formulation)	10 mg IV F0	5	1.7%
	30 mg IV F0	6	2.0%
	100 mg IV F0	6	2.0%
	100 mg SC F0	6	2.0%
	300 mg IV F0	12	4.1%
	300 mg SC F0	19	6.5%
	100 mg SC F2	6	2.0%
	75 mg SC F1	70	23.8%
	150 mg SC F1	91	31.0%
	300 mg SC F1	67	22.8%
	600 mg SC F1	6	2.0%
Pharmacokinetic Sampling	Intensive	102	34.3%
	Sparse	192	65.3%
	Mean	SD	Median (Range)
Age (yr)	36.3	12.8	37.0 (12-64)
Weight (kg)	86.1	22.1	83.4 (44-169)
BMI (kg/m^2)	29.1	7.3	27.7 (17.3-61.1)

[a] includes 4 subjects with no information about race

F0, F1 and F2 denote formulation strength, with values of 30 mg/mL,

100 mg/mL, and 100 mg/mL diluted to 30 mg/mL, respectively

AMG 317 Assay and Total Serum IgE Concentrations

Plasma samples were assayed for AMG 317 levels using a validated enzyme-linked immunosorbent assay (ELISA). Briefly, microplate wells were coated with recombinant human IL-4R:huFc reagent and then unknown, standard, and quality control (QC) samples were added. After the wells were incubated and washed, biotinylated recombinant human IL-4R:huFc was added to bind to the captured AMG 317. After the wells were incubated and washed, horseradish peroxidase (poly-HRP) streptavidin was added to the wells, which binds to the biotin label on the human IL-4R:huFc secondary reagent. After another washing step, tetramethylbenzidine (TMB) was added to the wells. In the presence of HRP, the TMB solution reacted with the peroxide to create a colorimetric signal that was proportional to the amount of AMG 317 bound by the capture reagent. The reaction was stopped, and the optical density was measured at 450 to 650 nm. The lower limit of quantification ranged from 9.7 to 10 ng/mL.

Total serum IgE levels were measured by standardized clinical chemistry tests.

Anti-AMG 317 Immunoassay

A validated electrochemiluminescence (ECL) immunoassay was used to detect anti-AMG 317 binding antibodies. The sensitivity of the assay was determined to be approximately 34.3 ng/mL of anti-AMG 317 in neat human serum. In the presence of 29 and 108 μg/mL of AMG 317, the assay can detect 94 and 500 ng/mL of antibody, respectively. Pooled normal human serum served as the negative control and an affinity-purified rabbit polyclonal anti-AMG 317 antibody served as the positive control. The mean ECL of each sample or control was divided by the mean ECL of the negative control to obtain the signal to noise (S/N) ratio. The mean ECL of the negative control was subtracted from the mean ECL of each sample or control to obtain the net ECL. The assay cut point was validated at an S/N of 1.17 (based on the upper bound of a one-sided 95% reference interval for the distribution of S/N values generated by serum samples from 56 healthy human serum donors). If the sample S/N was greater than the assay cut point, the sample was analyzed in the absence or presence of excess AMG 317 (confirmatory specificity testing). Reduction in the net ECL or S/N value of the drug-treated sample when compared to the untreated sample indicated that the sample contained drug-specific binding antibodies. A sample was reported as positive for anti-AMG 317 binding antibodies if the untreated sample S/N was greater than the assay cut point and the drug-treatment caused a percent net reduction in ECL greater than 50%, or if the untreated sample S/N was greater than the assay cut point and the drug-treated sample S/N was less than or equal to the assay cut point. The approximate relative concentration of anti-AMG 317 antibodies (antibody units) was determined by dividing the net ECL of each sample by the net ECL of the positive control (rabbit anti-AMG 317 at 1 μg/mL) and multiplying this ratio by the positive control concentration.

Pharmacokinetic Modeling

Noncompartmental Analysis

Noncompartmental PK analysis of subjects in Studies A and B was conducted using WinNonlin Professional (v 4.1e, Pharsight Corp.)

Population PK Base Structural Model

A two-compartment quasi-steady-state (QSS) approximation to the TMDD model (11) served as the structural model for population PK model development (Fig. 1). Previous population modeling of monoclonal antibodies has consistently demonstrated that a two-compartment model is necessary to characterize profiles from IV dosing (12–15). As AMG 317 targets a cell surface receptor, a mechanistic rationale exists for utilizing a target-mediated drug disposition model. The QSS approximation assumes that the binding rate is balanced by the sum of the dissociation and internalization rates (11). After exploratory analysis, the QSS model was selected because the entire range of concentrations could be described with the model. The parameters of the QSS model are listed in the caption of Fig. 1.

The population PK analysis was conducted using nonlinear mixed-effects modeling with NONMEM, Version VI, Level 2.0 and NONMEM, Version VII (ICON Development Solutions). The first-order conditional estimation method with interaction (FOCEI) was used. Model development was guided mostly by the diagnostic plots and plausibility of the parameter estimates with minimum objective function value (MOFV) as a secondary measure for model evaluation. Model validation took two steps: 1) a model was developed with AMG 317 concentration data from all studies except Study D, and 2) as a model

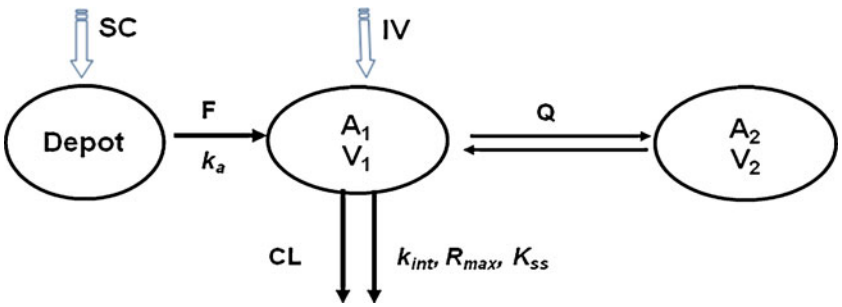

Fig. 1 Schematic of the population PK model with parallel linear and non-linear clearance (CL), characterized by the QSS parameters k_{int}, R_{max} and K_{ss}. k_{int} is the internalization rate constant of drug-receptor complex, R_{max} is the total receptor concentration (assumed to be a constant parameter of the system), K_{SS} is the QSS constant equal to $(k_{int} + k_{off})/k_{on}$ where k_{off} is the dissociation rate constant of drug-receptor complex. A_1 and A_2 represent the amount of drug, and V_1 and V_2 represent the volumes of distribution of the central and peripheral compartments, respectively. Q is the intercompartmental clearance. AMG 317 was administered either into the central compartment by IV administration or into a depot compartment by SC injection. F is SC bioavailability, and k_a is the rate of absorption from the SC compartment.

evaluation step, the observed data in Study D were compared with the predicted based on the final model from 1) using the covariate information in patients of Study D. When the predicted were consistent with observed, final parameter values were estimated with the model in 1) from all data.

All inter-individual random effects were described by an exponential model, $\exp(\eta)$, where η is normally distributed with mean 0 and an unknown variance to be estimated. The residual error model was described by combined additive and exponential error on log-transformed concentrations. The residual error was assumed to be distributed according to a standard normal distribution with mean 0.

Covariate Analysis

The functional form of multipliers in the covariate model for continuous function covariates was $\left(\frac{\mathrm{COV}}{\mathrm{COV_{ref}}}\right)^{\theta}$. The reference values of $\mathrm{COV_{ref}}$ were 80 kg for body weight and 40 years for age. The exponent, θ, for dependence on weight was fixed to a value of 0.75 on clearance (CL), 1 on volume (V_1), and was estimated for other covariates, e.g., age on k_a. For dichotomous covariates (such as for formulation, route, or anti-drug antibody) the functional form was θ^x with x taking values of 0 or 1 and $\theta>0$ to be estimated. For the anti-drug effect on CL and the total receptor concentration (R_{max}), an equivalent form of $1+(\theta_{CLABS}-1)\cdot$ABS was coded with θ_{CLABS} representing the increase in CL in the presence of anti-drug antibodies, where ABS was the antibody status and assigned a value of 0 if negative and 1 if positive. During the first two weeks it is believed that the anti-drug antibodies (if present) would be immature and less likely to impact PK and PD. Therefore, ABS was assumed to be negative within two weeks of the first dose; if antibody status was negative at a timepoint but the previous and successive measurements were positive, ABS was coded as positive.

Model Evaluation

The base, final, and important intermediate models were evaluated with a set of diagnostic tools. The evaluation included plots of observed AMG 317 concentrations *versus* population and individual predictions, weighted residuals *versus* time and population predictions, observed concentrations, population and individual predictions *versus* time, histograms and quantile-quantile plots of the individual random-effect distributions, scatter-plot matrix of the individual random effects, random effects *versus* continuous covariates, and distributions of individual random effects stratified by the categorical covariates.

For each individual random effect, the shrinkage was computed as $1-\mathrm{var}(\eta_{ind})/\Omega$, where η_{ind} and Ω are the *post hoc* individual random effect and the estimated population variance parameter for a PK parameter of interest. A similar but different definition is described in Savic (16). Low shrinkage values indicate that the majority of subjects have enough data to estimate their individual PK parameters.

The precision of model parameters was investigated by the bootstrap method. More concretely, 500 replicate datasets were generated through random sampling with replacement using the individual as the sampling unit (17,18). Stratification during the random sampling process was implemented to ensure that the bootstrap datasets adequately represent the original data with respect to continuous covariate distributions and categorical covariate percentages. Non-parametric, empirical 90% confidence intervals (CI) were constructed by observing the 5th and 95th quantiles of the resulting parameter distributions for the bootstrap runs that provided parameter estimates.

Exposure-Response Modeling

Individual *post hoc* parameter estimates from the final PK model were used to obtain predicted cumulative area under the curve (CAUCT) at each measured IgE time point. In addition, the areas under the curve (AUCs) of 7, 14, 21, and 28 days prior to the IgE time points were computed. We referred to these AUCs as AUC7, AUC14, AUC21 and AUC28, respectively. Linear mixed effects modeling was performed in patients whose baseline IgE was greater than healthy volunteers, to relate each of AMG 317 exposure measures (i.e., CAUCT, AUC7, AUC14, AUC21, and AUC28) to IgE levels. In order to compare across different AMG 317 exposure measures as predictors, only IgE observations for which all the predicted exposure measures were available were included in the analysis. For instance, if AUC of 28 days prior to the observed IgE was missing, that record was excluded. One record with IgE level of 0 was also excluded.

The models were fitted to log-transformed IgE and exposure measures with data from patients in Phase 2 study. All model parameters were estimated using maximum likelihood method. Model comparisons were made using Akaike information criterion (AIC) and standard errors of estimates.

Other models such as an indirect response type were explored, but the model fit appeared to be poor, and predictions from the indirect response model did not agree with observed data.

RESULTS

Profiles from single dose IV and multiple dose SC cohorts from the studies with intensive PK sampling illustrate the

nonlinearity of AMG 317 pharmacokinetics (Fig. 2). Following IV bolus and infusion dosing in healthy subjects, AUC_{last} increased by approximately 6.5- and 13-fold over the dose range of 10 to 30 mg, and 100 to 1000 mg, respectively (Table II). After weekly SC dosing, $AUC_{168\ h}$ at week 3 increased by 30-fold from 75 to 600 mg (Table III). Therefore, it was deemed necessary to incorporate a nonlinear component in pharmacokinetic compartmental modeling of AMG 317 PK over this range of doses.

Population Pharmacokinetic Modeling

Although the base model ran successfully, the final model, as well as the majority of intermediate and bootstrap models, had terminated runs with rounding errors. However, all parameter estimates of these failed runs appeared to be reasonable and consistent. No issues were detected from the diagnostic plots that would cause concern. Therefore, in this work the MOFV and the associated likelihood ratio tests were considered only secondary in the list diagnostic measures.

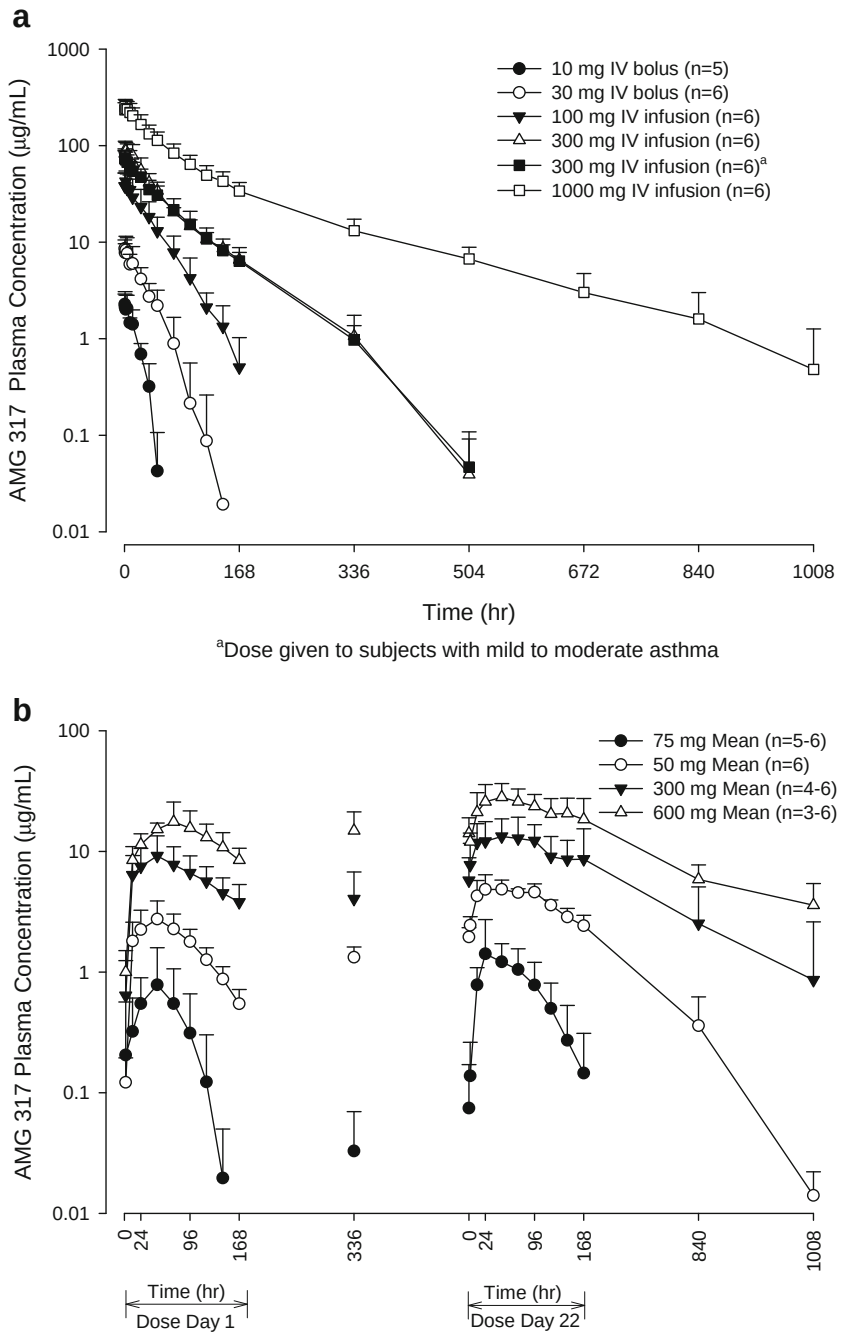

Fig. 2 (**a**) Plasma AMG 317 concentration-time profiles in humans after a single IV dose (Study A). (**b**) Plasma AMG 317 concentration-time profiles in humans after four weekly SC doses (Study B).

Table II Noncompartmental Analysis of Single IV Dose Pharmacokinetics (Study A). t_{max} Reported as Median (range). All Other Parameters Reported as Mean (SD). HV—Healthy Volunteers, MMA—Subjects with Mild to Moderate Asthma

Dose (mg)	Route	n	Patient Status	Dose Day	t_{max} (hr)	C_{max} or C_0 (μg/mL)	AUC_{last} (μg·hr/mL)	AUC_{last}/Dose (μg·hr/mL)/mg
10	IV bolus	5	HV	1	0	2.70	40.1	4.01
					(0–1.0)	(0.835)	(12.4)	(1.24)
30	IV bolus	6	HV	1	0	10.4	260	8.67
					(0–4.0)	(3.35)	(114)	(3.80)
100	IV infusion	6	HV	1	1.5	46.1	1660	16.6
					(0.5–12)	(14.4)	(699)	(7.0)
300	IV infusion	6	HV	1	0.8	93.9	5050	16.8
					(0.5–12)	(20.9)	(1010)	(3.4)
300	IV infusion	6	MMA	1	0.5	74.0	4520	15.1
					(0.5–1.0)	(15.4)	(1250)	(4.2)
1000	IV infusion	6	HV	1	1.0	260	22200	22.2
					(0.5–2.0)	(48.5)	(5670)	(5.7)

A two-compartment QSS model was selected as the structural model. Preliminary investigations with a Michaelis-Menten approximation of the non-linear clearance exhibited systematic bias in estimation at concentrations below 300 ng/mL; the bias was eliminated with the QSS approximation of TMDD (not shown). Therefore, the QSS model with random effects on CL, V_1, Q, k_a, and R_{max} was selected as the base model for exploration of the PK-covariate relationships.

The subjects in this study had a median body weight of 83.4 kg with the body weight ranging from 44 to 169 kg. The median age was 37 years with a range of 12 to 64 years (Table I). For covariate investigations, random effects on clearance and central volume indicated dependence on

Table III Noncompartmental Analysis of Multiple Dose Pharmacokinetics on Days 1 and 22 After Weekly SC Administration of AMG 317 (Study B). t_{max} Reported as Median (range). All Other Parameters Reported as Mean (SD). MMA—Subjects With Mild To Moderate Asthma

Dose (mg)	Route	Patient Status	n	Dose Day	t_{max} (hr)	C_{max} or C_0 (μg/mL)	$AUC_{168\ h}$ (μg·hr/mL)	$AUC_{168\ h}$/Dose (μg·hr/mL)/mg	AUC_{ratio}
75	SC bolus	MMA	6	1	24	0.873	55.3	0.74	
					(2.0–72)	(0.763)	(49.2)	(0.66)	
			6	22	48	1.60	126	1.68	3.93
					(24–48)	(1.24)	(60.8)	(0.8)	(4.04)
150	SC bolus	MMA	6	1	48	2.77	280	1.87	
					(24–72)	(1.12)	(92.8)	(0.62)	
			6	22	36	5.66	667	4.45	2.64
					(24–96)	(0.753)	(67.2)	(0.4)	(0.96)
300	SC bolus	MMA	6	1	49	9.59	1050	3.50	
					(48–97)	(4.31)	(348.0)	(1.16)	
			5	22	71	14.4	1810	6.03	1.87
					(47–170)	(6.59)	(760)	(2.5)	(0.47)
600	SC bolus	MMA	6	1	73	19.1	2130	3.55	
					(23–96)	(6.88)	(528)	(0.88)	
			5	22	48	29	3810	6.35	1.75
					(24–73)	(9.1)	(1130)	(1.9)	(0.316)

body weight. A stepwise forward selection method was used that resulted in the addition of body weight effect on CL and V_1 with reduction and increase in MOFV by 257 and 15 points, respectively, and age effect on k_a with a reduction in MOFV further by 100 points. This model appeared to have adequately accounted for the dependencies of the random effects on age and weight, judging from the diagnostics. The effect of age on k_a was significant and moderately strong, with the exponent estimated as –0.7, showing greater absorption in younger subjects. However, effects of formulation and route of administration on central volume were also evident. The final covariate model included these two effects explicitly. Subjects administered the 100 mg/mL formulation exhibited lower central volume than the 30 mg/mL formulation.

No effect of sex on CL and V_1 was found, nor was the race effect on the PK parameters discerned after including effects of body weight. However, the number of subjects in each of the non-white racial categories was small (Table I). Replacement of body weight by the fat-free mass, lean body weight, body surface area, or ideal body weight was also tested. The diagnostic plots indicated that these body-size measures were not able to describe the increase of central volume observed in the heavier patients.

The influence of anti-AMG 317 antibodies was investigated graphically and by explicit inclusion in the model. AMG 317 concentrations were slightly lower in subjects with positive anti-AMG 317 antibodies. When antibody status was evaluated as a covariate on various PK parameters, it was significant for CL and R_{max} from the likelihood ratio test. The presence of anti-drug antibodies was associated with a 16% increase in CL; for R_{max} the magnitude of the effect was small at 6%, and the 90% confidence interval from bootstrap shows non-significance (Table IV).

The final population PK model included random effects on CL, V_1, Q, k_a, and R_{max} with covariate effects of body weight on CL and V_1, age on k_a, formulation and route effects on V_1, and antibody status effect on CL and R_{max} (Table IV).

Table IV Parameter Estimates from the Final Population PK Model

Model Term	Parameter	Estimate	90% Confidence Intervals
$CL = \theta_{CL} \cdot (WT/80)^{0.75} \cdot [1 + (\theta_{CL,ABS} - 1) \cdot ABS] \cdot \exp(\eta_{CL})$	θ_{CL} (mL/hr)	35.0	(34.6, 36.9)
	$\theta_{CL,ABS}$	1.16	(1.01, 1.26)
	$SD(\eta_{CL})$	0.40	(0.37, 0.43)
$V_1 = \theta_{V1} \cdot (WT/80) \cdot \theta_{V1,FORM}^{FORM} \cdot \theta_{V1,ROUT}^{(1-ROUT)} \cdot \exp(\eta_{V1})$	θ_{V1} (L)	1.78	(1.70, 1.80)
	$\theta_{V1,FORM}$	0.54	(0.34, 0.77)
	$\theta_{V1,ROUT}$	2.03	(1.83, 2.22)
	$SD(\eta_{V1})$	0.28	(0.25, 0.29)
$V_2 = \theta_{V2}$	θ_{V2} (L)	5.03	(4.89, 5.34)
$Q = \theta_{Q} \cdot \exp(\eta_{Q})$	θ_{Q} (mL/hr)	27.4	(26.1, 28.7)
	$SD(\eta_{Q})$	0.44	(0.44, 0.53)
$K_{SS} = \theta_{KSS}$	θ_{KSS} (ng/mL)	51.7	(48.3, 52.7)
$K_{int} = \theta_{Kint}$	θ_{Kint} (1/hr)	0.167	(0.164, 0.172)
$R_{max} = \theta_{Rmax} \cdot [1 + (\theta_{Rmax,ABS} - 1) \cdot ABS] \cdot \exp(\eta_{Rmax})$	θ_{Rmax} (ng/mL)	304	(302, 322)
	$\theta_{Rmax,ABS}$	1.06	(0.99, 1.15)*
	$SD(\eta_{Rmax})$	0.24	(0.20, 0.24)
$K_a = \theta_{Ka} \cdot (AGE/40)^{\theta Ka,AGE} \cdot \exp(\eta_{ka})$	θ_{Ka} (1/hr)	0.0077	(0.007, 0.0078)
	$\theta_{Ka,AGE}$	-0.72	(-0.83, -0.59)
	$SD(\eta_{Ka})$	0.38	(0.32, 0.40)
$F_1 = \theta_{F1}$	θ_{F1}	0.243	(0.234, 0.250)
$Y = F.\exp\left(\sqrt{\frac{\theta_{ae}}{F^2} + \theta_{pe}}.\exp(\eta_{BSV}).\varepsilon_1\right)$	$SD(\theta_{pe})$	0.18	(0.17, 0.19)
	$SD(\theta_{ae})$ (ng/mL)	36.4	(33.9, 38.3)
	$SD(\eta_{BSV})$	0.407	(0.375, 0.444)

* Not significant

WT and AGE are continuous variables of patients' baseline body weight and age, respectively.

ROUT is an indicator variable with values of 0 and 1 to denote intravenous and subcutaneous routes of administration, respectively. FORM is an indicator variable for formulation strength, with values of 0 (30 mg/mL), 1 (100 mg/mL), 2 (100 mg/mL diluted to 30 mg/mL). ABS, an indicator variable for anti-AMG 317 antibody status, is 1 for positive incidence and 0 otherwise.

ae: additive error; *pe*: proportional error; *BSV*: between subject variability; $\varepsilon_1 \sim N(0,1)$

Basic goodness-of-fit plots of the final model (Fig. 3) demonstrated that the weighted residuals are evenly distributed around the line of identity, and there is no obvious systematic bias in residuals with time or concentration. The random effects were close to being normally distributed and were not correlated. Compared with the base model, the final model has a lower MOFV by approximately 350 points, and the *post hoc* estimates of PK parameters showed lower correlations with covariates. Shrinkage of the random effects for the final model was moderate at 40-65%, indicating that the data were overall not too sparse to estimate individual PK parameters. The coefficient of variation as approximated by the standard deviation of the proportional error (θ_{PE}) in the error model was 18%, and the standard deviation of the additive error (θ_{AE}) was 36.4 ng/mL.

Model Validation and Simulations

Validation by data splitting was conducted by fitting the covariate model to concentration data from three of the four studies (N=102). Predictions for subjects in the excluded study (D, N=193) then were generated from model parameters derived from the other three studies. The model was found to be in reasonably good agreement with the observed data except for some bias at higher concentrations (Supplementary Material, Figure S1). The PK parameter estimates were later compared with those of the final model based on all data. The absolute percent differences for most of the fixed-effect parameters were less than 5% (except for V_2 and K_{ss}: absolute percent differences were 10% and 11%, respectively).

The final PK parameters from modeling all 294 subjects and the empirical 90% confidence interval from 500 bootstrap replicates are included in Table IV. For each of the PK parameters, the empirical cumulative distribution function was not distinguishable between the first 400 runs and the final 500 runs, which shows the adequacy of 500 as the bootstrap sample size.

Exposure-Response Modeling

The dose-response relationship for Phase 2 study is illustrated in Fig. 4a for weekly SC doses. The median observed

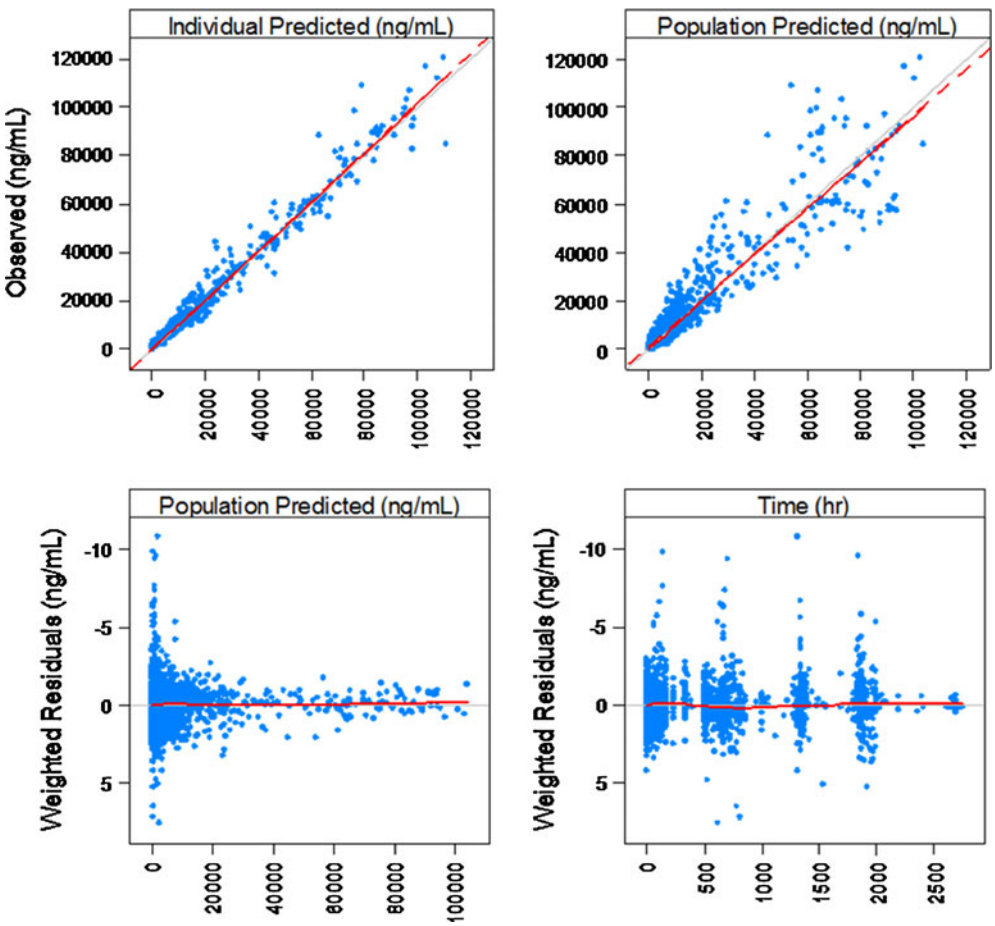

Fig. 3 Final Model Goodness-of-Fit Plots (top left) observed AMG 317 concentrations (ng/mL) *vs* individual predicted concentrations; (top right) observed AMG 317 concentrations (ng/mL) *vs*. population predicted concentrations. The solid grey lines are lines of unity and the red solid and dotted lines are lines of trend and linear regression, respectively; (bottom left) weighted residuals *vs* population predicted concentrations; (bottom right) weighted residuals *vs* time. The thin solid grey lines are the lines of zero residuals, and the thick red lines represent the trend of all points.

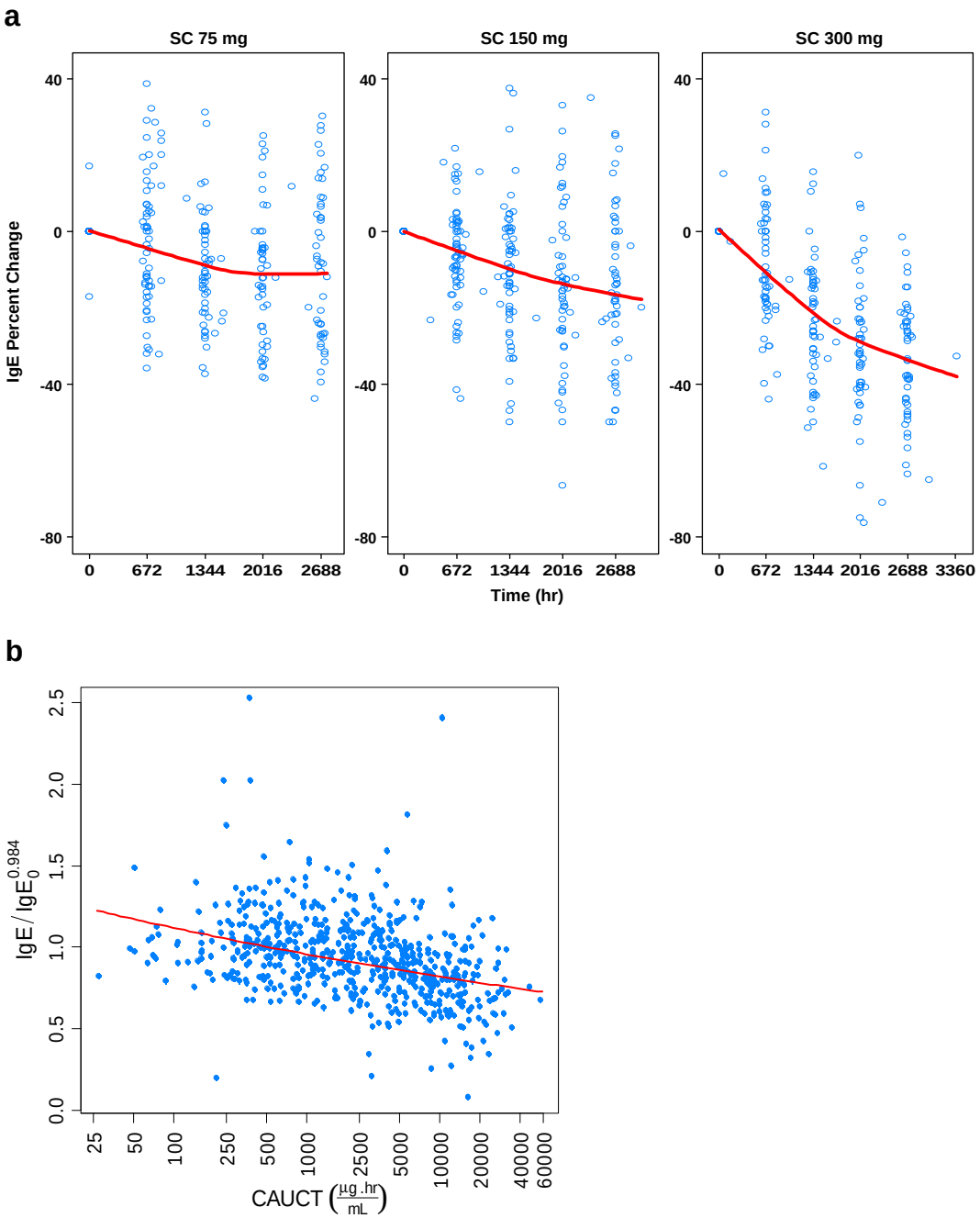

Fig. 4 (**a**) IgE response at AMG 317 doses of 75, 150 and 300 mg (percent change from baseline *versus* time after start of treatment). Observed data from the Phase 2 study (Study D) are shown in blue, solid red lines are the trend lines provided by the lowess smoother function. (**b**) IgE response (ratio of IgE and IgE at baseline) as a continuous function of AMG 317 exposure (cumulative AUC to time T, CAUCT).

decrease from baseline at month 4 (2688 h) was 7%, 14%, and 34% for doses of 75, 150 and 300 mg, respectively.

The median baseline IgE levels in patients from all studies were higher than in healthy subjects by 2.9-fold, and the difference was significant (p-value < 0.0002). The final population PK model was used to generate *post hoc* estimates of AMG 317 exposure metrics for each patient as described in the methods. The best model relating exposure to IgE response was a linear model in logarithmic scale that included baseline IgE (IgE_0) and CAUCT as the treatment effect Eq. 1. Random effects included between-subject variability (BSV) in the intercept and the slope for IgE_0 (η) and residual variability (ε). Diagnostic plots (Supplementary Material, Figure S2) indicated adequate model fit with no apparent bias and no random-effect and error heteroskedasticity that would

call for concern. The treatment effect was highly significant (p-value < 0.0001).

$$\log(\mathrm{IgE}) = 0.894 + \eta_1 + (0.984 + \eta_2) \cdot \log(\mathrm{IgE}_0) - 0.068 \cdot \log(\mathrm{CAUCT}) + \varepsilon, \quad (1)$$

where (η_1, η_2) are jointly normal with mean 0, variances (0.40,0.014) and correlation -0.98, and $\varepsilon \sim N(0,0.0429)$.

A plot of CAUCT *versus* $\mathrm{IgE}/\mathrm{IgE}_0^{0.984}$ is shown in Fig. 4b, where $\mathrm{IgE}/\mathrm{IgE}_0^{0.984}$, close to the proportion to the baseline, can be thought of as baseline-corrected IgE.

DISCUSSION

Traditional therapy for asthma consists of inhaled corticosteroids and beta-2 agonists, with more severe disease or disease flares treated with systemic corticosteroids. More recently, the humanized monoclonal antibody omalizumab was approved as an option for treatment of moderate to severe asthma in patients whose disease is inadequately controlled with corticosteroids (19). Omalizumab forms complexes with IgE and interrupts the allergic cascade triggered by free IgE. The fully human monoclonal antibody AMG 317 targets another point of intervention in the pathogenesis of asthma through blockade of the IL-4Rα, a common receptor for IL-4 and IL-13. These cytokines play a critical role in a Th2-mediated inflammatory response to allergens, including immunoglobulin class switching from IgG to IgE, activation of mast cells, recruitment of eosinophils and neutrophils, and airway hyper-responsiveness (1). Therapeutics targeted against IL-4, IL-13 or IL-4Rα represent a possible novel mechanism of action for asthma treatments. Other biologics besides AMG 317 that are targeted to this pathway and under development are pitrakinra, a dual IL-4 and IL-13 antagonist (20), and CAT-354, a human monoclonal antibody that binds and neutralizes IL-13 (21).

By means of population PK analysis of early phase clinical trials of AMG 317, we have conducted a comprehensive modeling evaluation of intensive and sparse PK data obtained in healthy volunteers and asthma patients (N=295) from both IV and SC routes of administration. SC bioavailability was 24.3%, and absorption was slow with an absorption half-life of 3.8 days. Absorption rate decreased with age. It was 62% higher for a 20-year-old than for a 40-year-old subject. This is the first example known to us of a covariate effect of age on absorption rate of monoclonal antibodies. This finding raises the possibility of a decrease in lymphatic flow with age, as absorption of antibodies from the subcutaneous space into systemic circulation occurs largely by lymphatic absorption (22).

The population PK model yielded an estimate of linear clearance for an 80 kg, 40-year-old subject of 35.0 mL/hr (90% confidence interval: (34.6, 36.9) mL/hr) following IV injection and 144 mL/hr following SC injection. The only approved human IgG_2 is panitumumab, which has an IV clearance of 11.4 mL/hr (15). CAT-354, like AMG317, is intended for IV injection to treat asthma. A human IgG_4, it has a clearance of ~8 mL/hr (21). Omalizumab, the only approved MAb for asthma, is a humanized IgG_1 targeted to IgE (1). It has a SC clearance of 13.2 mL/hr (24). Hence, AMG 317 is relatively rapidly cleared in comparison to other fully human monoclonal antibodies of the same isotype or for the same indication. On the other hand, AMG 317 SC clearance is more than 100-fold lower than that of pitrakinra, a 15-kDa biologic that is targeted to the same pathway as AMG-317 (20).

The central and peripheral volumes of distribution of AMG 317 are 1.78 and 5.03 L, respectively, for a total volume of 6.81 L, comparable to the volumes reported for other IV-administered human or humanized monoclonal antibodies. For example, panitumumab, golimumab and trastuzumab have total volumes of distribution of 6.54, 6.75, and 7.74 L, respectively (12,15,23). However, they is larger than the 4.0 L volume of distribution of IV-administered CAT-354 (21). The total volume divided by SC bioavailability of AMG 317 (6.81 L/0.243 = 28 L) is considerably higher than 3.63 L, which is the total volume divided by bioavailability of omalizumab (24). On the other hand, AMG 317 has a much lower V/F than that of pitrakinra at 67.5 L (20). This is expected because pitrakinra has a molecular mass of only 15 kD and, as such, is less hindered in its movement in the interstitial space (25) compared to AMG 317, which as an IgG_2 has a molecular mass of 150 kD. An allometric model for linear clearance and central volume with fixed exponents of 0.75 for clearance and 1.0 for volume (26,27) adequately described the dependence on body weight. K_{ss} was 51.7 ng/mL (90% confidence interval: (48.3, 52.7 ng/mL), about twice the value of the AMG 317 dissociation constant ($K_D = 1.8 \times 10^{-10}$ M or 27 ng/mL).

Previously published population PK models of monoclonal antibodies model data from only one route of administration, either IV or SC (e.g (12,13,15,23,24,28)). From models of IV data, it is evident that monoclonal antibody pharmacokinetics follows a biphasic distribution, but it is often difficult to discern this from only SC data. Our modeling analysis included simultaneous fit of both IV and SC data across a large range of doses. An unexpected covariate that was identified was route of administration on central volume, the volume being about twice as high for the IV route compared to the SC route, even after accounting for bioavailability. We do not have a physiological explanation for such a finding, but a similar type of route dependency, with a higher predicted central volume from IV dosing was found when simultaneously fitting IV and oral PK data on a small molecular weight drug, cilobradine (29). A model with formulation effect on bioavailability (rather than on the

central volume) was tested. While this model is more biologically plausible than the model with formulation effect on the central volume, it was not able to account for the observed formulation differences. This finding indicates that the same SC dose (but different formulation strength) of monoclonal antibody administered does not yield the same pharmacokinetic profile.

The population PK model allowed estimation of individual drug exposure for subjects in the Phase 2 trial for whom only sparse PK samples were obtained. The estimates could then be examined against measures of individual pharmacological response. Other biomarkers such as sputum eosinophil counts, exhaled nitric oxide, lung function tests, and corticosteroid usage were exploratory endpoints in one or more studies, but the only biomarker collected across all four studies was total serum IgE. Hence, other biomarkers relevant to the Th2 pathway were not explored. IgE was used as a biomarker because it is a known effector molecule in the Th2 pathway, its production is increased when IL-4Rα is activated, and crosslinked IgE has a direct role in mast cell degranulation (30). Total serum IgE was obtained at baseline and at approximate monthly intervals. A decrease in IgE levels relative to baseline was observed following chronic weekly injection of AMG 317. The intensity of the response increased with both dose and duration of dosing. By utilizing the population PK model to generate *post hoc* estimates of exposure, data from all the trials could be condensed into a single exposure-response relationship. A significant treatment effect on the change in IgE levels was observed when the IgE response was modeled with CAUCT as the dependent variable. Sustained SC AMG 317 dosing over several months appears to be necessary for a relatively modest IgE response. Omalizumab has activity limited to sequestering IgE and produces reduction in free IgE levels to the range of 10-20 IU/mL, much lower than levels attained with AMG 317 (geometric mean IgE at 16 weeks was 128 IU/mL for the 300 mg SC dose).

In conclusion, a comprehensive population PK modeling analysis was conducted on IV and SC data obtained from four early phase trials of AMG 317 to evaluate its pharmacokinetics in healthy volunteers and patients with mild to severe asthma. The model revealed several variables that contribute to inter-individual variation and illustrated that a quantitative exposure-response relationship exists between cumulative exposure and changes in IgE levels.

REFERENCES

1. Wagelie-Steffen AL, Kavanaugh AF, Wasserman SI. Biologic therapies for the treatment of asthma. Clin Chest Med. 2006;27:133–47. vii.
2. Grünig G, Warnock M, Wakil AE, Venkayya R, Brombacher F, Rennick DM, *et al.* Requirement for IL-13 independently of IL-4 in experimental asthma. Science. 1998;282:2261–3.
3. Wills-Karp M, Luyimbazi J, Xu X, Schofield B, Neben TY, Karp CL, *et al.* Interleukin-13: central mediator of allergic asthma. Science. 1998;282:2258–61.
4. Webb DC, McKenzie AN, Koskinen AM, Yang M, Mattes J, Foster PS. Integrated signals between IL-13, IL-4, and IL-5 regulate airways hyperreactivity. J Immunol. 2000;165:108–13.
5. Kelly-Welch AE, Melo MEF, Smith E, Ford AQ, Haudenschild C, Noben-Trauth N, *et al.* Complex role of the IL-4 receptor alpha in a murine model of airway inflammation: expression of the IL-4 receptor alpha on nonlymphoid cells of bone marrow origin contributes to severity of inflammation. J Immunol. 2004;172:4545–55.
6. Hershey GK, Friedrich MF, Esswein LA, Thomas ML, Chatila TA. The association of atopy with a gain-of-function mutation in the alpha subunit of the interleukin-4 receptor. N Engl J Med. 1997;337:1720–5.
7. van der Pouw Kraan TC, van Veen A, Boeije LC, van Tuyl SA, de Groot ER, Stapel SO, *et al.* An IL-13 promoter polymorphism associated with increased risk of allergic asthma. Genes Immun. 1999;1:61–5.
8. Graves PE, Kabesch M, Halonen M, Holberg CJ, Baldini M, Fritzsch C, *et al.* A cluster of seven tightly linked polymorphisms in the IL-13 gene is associated with total serum IgE levels in three populations of white children. J Allergy Clin Immunol. 2000;105:506–13.
9. Suzuki K, Nakajima H, Watanabe N, Kagami SI, Suto A, Saito Y, *et al.* Role of common cytokine receptor gamma chain (gamma (c))- and Jak3-dependent signaling in the proliferation and survival of murine mast cells. Blood. 2000;96:2172–80.
10. Corren J, Busse W, Meltzer EO, Mansfield L, Bensch G, Fahrenholz J, *et al.* A randomized, controlled, phase 2 study of AMG 317, an IL-4Ralpha antagonist, in patients with asthma. American journal of respiratory and critical care medicine. 2010;181:788–96.
11. Gibiansky L, Gibiansky E, Kakkar T, Ma P. Approximations of the target-mediated drug disposition model and identifiability of model parameters. J Pharmacokinet Pharmacodyn. 2008;35:573–91.
12. Bruno R, Washington CB, Lu JF, Lieberman G, Banken L, Klein P. Population pharmacokinetics of trastuzumab in patients with HER2+ metastatic breast cancer. Cancer Chemother Pharmacol. 2005;56:361–9.
13. Xu Z, Seitz K, Fasanmade A, Ford J, Williamson P, Xu W, *et al.* Population pharmacokinetics of infliximab in patients with ankylosing spondylitis. J Clin Pharmacol. 2008;48:681–95.
14. Dirks NL, Nolting A, Kovar A, Meibohm B. Population pharmacokinetics of cetuximab in patients with squamous cell carcinoma of the head and neck. J Clin Pharmacol. 2008;48:267–78.
15. Ma P, Yang BB, Wang YM, Peterson M, Narayanan A, Sutjandra L, *et al.* Population pharmacokinetic analysis of panitumumab in patients with advanced solid tumors. J Clin Pharmacol. 2009;49:1142–56.
16. Savic RM, Karlsson MO. Importance of shrinkage in empirical bayes estimates for diagnostics: problems and solutions. The AAPS journal. 2009;11:558–69.
17. Efron B. Missing data, imputation, and the bootstrap. J Am Stat Assoc. 1994;89:463–79.
18. Parke J, Holford NH, Charles BG. A procedure for generating bootstrap samples for the validation of nonlinear mixed effects population models. Comput Methods Programs Biomed. 1999;59:19–29.
19. Humbert M, Beasley R, Ayres J, Slavin R, Hébert J, Bousquet J, *et al.* Benefits of omalizumab as add-on therapy in patients with

severe persistent asthma who are inadequately controlled despite best available therapy (GINA 2002 step 4 treatment): INNOVATE. Allergy. 2005;60:309–16.
20. Getz EB, Fisher DM, Fuller R. Human pharmacokinetics/pharmacodynamics of an interleukin-4 and interleukin-13 dual antagonist in asthma. The Journal of Clinical Pharmacology. 2009;49:1025–36.
21. Singh D, Kane B, Molfino N, Faggioni R. A phase 1 study evaluating the pharmacokinetics, safety and tolerability of repeat dosing with a human IL-13 antibody (CAT-354) in subjects wtih asthma. BMC Pulmonary Medicine. 2010;10:3–11.
22. Thygesen P, Macheras P, Van Peer A. Physiologically-based PK/PD modelling of therapeutic macromolecules. Pharm Res. 2009;26:2543–50.
23. Zhou H, Jang H, Fleischmann RM, Bouman-Thio E, Xu Z, Marini JC, *et al.* Pharmacokinetics and safety of golimumab, a fully human anti-TNF-alpha monoclonal antibody, in subjects with rheumatoid arthritis. J Clin Pharmacol. 2007;47:383–96.
24. Hayashi N, Tsukamoto Y, Sallas WM, Lowe PJ. A mechanism-based binding model for the population pharmacokinetics and pharmacodynamics of omalizumab. Br J Clin Pharmacol. 2007;63:548–61.
25. Jain RK. Vascular and interstitial barriers to delivery of therapeutic agents in tumors. Cancer Metastasis Rev. 1990;9:253–66.
26. Boxenbaum H. Interspecies pharmacokinetic scaling and the evolutionary-comparative paradigm. Drug metabolism reviews. 1984;15:1071–121.
27. Mordenti J, Chen SA, Moore JA, Ferraiolo BL, Green JD. Interspecies scaling of clearance and volume of distribution data for five therapeutic proteins. Pharm Res. 1991;8:1351–9.
28. Sun YN, Lu JF, Joshi A, Compton P, Kwon P, Bruno RA. Population pharmacokinetics of efalizumab (humanized monoclonal anti-CD11a antibody) following long-term subcutaneous weekly dosing in psoriasis subjects. J Clin Pharmacol. 2005;45:468–76.
29. Fliss G, Staab A, Tillmann C, Trommeshauser D, Schaefer HG, Kloft C. Population Pharmacokinetic Data Analysis of Cilobradine, an I f Channel Blocker. Pharm Res. 2008;25:359–68.
30. Segal DM, Taurog JD, Metzger H. Dimeric immunoglobulin E serves as a unit signal for mast cell degranulation. Proceedings of the National Academy of Sciences of the United States of America. 1977;74:2993–7.